

Performance assessment of RC frame designed using force, displacement & energy based approach

Onkar G. Kumbhar^a and Ratnesh Kumar*

Department of Applied Mechanics, Visvesvaraya National Institute of Technology,
Nagpur 440010, Maharashtra, India

(Received July 7, 2019, Revised September 26, 2019, Accepted November 12, 2019)

Abstract. Force based design (FBD) approach is prevalent in most of the national seismic design codes world over. Direct displacement based design (DDBD) and energy based design (EBD) approaches are relatively new methods of seismic design which claims to be more rational and predictive than the FBD. These three design approaches are conceptually distinct and imparts different strength, stiffness and ductility property to structural members for same plan configuration. In present study behavioural assessment of frame of six storey RC building designed using FBD, DDBD and EBD approaches has been performed. Lateral storey forces distribution, reinforcement design and results of nonlinear performance using static and dynamic methods have been compared. For the three approaches, considerable difference in lateral storey forces distribution and reinforcement design has been observed. Nonlinear pushover analysis and time history analysis results show that in FBD frame plastic deformation is concentrated in the lower storey, in EBD frame large plastic deformation is concentrated in the middle storeys though the inelastic hinges are well distributed over the height and, in DDBD frame plastic deformation is approximately uniform over the height. Overall the six storey frame designed using DDBD approach seems to be more rational than the other two methods.

Keywords: force based design; direct displacement based design; energy based design; target drift; seismic behavior; nonlinear analysis

1. Introduction

Damage to structural and non-structural elements during past earthquakes steered structural engineers and researchers to work on new rational design methods. It is expected that the new design methods shall be capable of controlling the possible damage in structure efficiently and enhance its seismic performance. The development in seismic design started from force-based approach and presently moving towards more rational performance-based approaches like displacement-based design and energy-based design. Even though from early researches during (1920) the interpretation of inertial action during seismic event was well understood, however, the quantification of exact seismic force was not possible. Moreover, the buildings designed for lateral wind loads performed better during seismic events occurred in 1920s and early 1930s (Priestley *et al.* 2007). Hence, structural engineers inferred that structures in seismic regions can be designed for some lateral force in proportion to the mass of the structure, similar to wind loads. Therefore, in early 20th century seismic force evaluation for structure was proportional to mass of structure (i.e. typically 10 percent of weight of structure) irrespective to its dynamic properties. Further in 1940s and 50s, effect of structural stiffness in terms of its period of vibration was incorporated in design but structural

analysis was based on elastic response procedures. However, in early 1960 the measurement of actual earthquakes indicated that the seismic force in case of a high intensity earthquake imparts much larger force than the anticipated 10 percent of the weight of structure. However, it was observed by researchers that the cyclic nature of earthquake can be utilized in designing economical structures by imparting ductility. It was also understood that the utilization of ductility in RC structure will impart significant damage, however, due to rare occurrence of earthquake designers accepted the risk. Later experimental and empirical results indicated that a ductile detailed structure survive higher level of ground shaking than predicted/designed level, hence ductility considerations were introduced in the design during 1960's and 70's. Further, importance of strength parameter to control drift level and indirectly to reduce damage potential during expected level earthquake was realized in 1980s and 90s (Priestley *et al.* 2007). Presently the 'Force-Based Design' (FBD) approach is well-established procedure and prescribed by most of the seismic design national codes. In FBD, anticipated elastic forces are reduced by response reduction/modification factor (ATC 19, 1995). This reduction is based on implicit reserve parameters i.e., over strength, ductility, redundancy and damping (Whittaker and Rojahn 1999, Kappos 1999, Borzi and Elnashai 2000, Lakhade *et al.* 2018). In fact, when subjected of the anticipated seismic hazard the members of the FBD designed building are expected to undergo inelastic deformation, however, these buildings are expected to grossly behave in desired manner due to aforementioned

*Corresponding author, Associate Professor
E-mail: ratnesh.eq@gmail.com

^a Ph.D. Student

implicit reserve parameters. Moreover, for important lifeline buildings (like Hospital), to achieve the better performance, FBD procedure uses higher “Importance Factor” which is in fact a force enhancement factor. In addition to this, FBD procedure recommends checking the elastic displacement of the structure to deform within the prescribed limiting value. Overall, the exact inelastic behavior of the building designed using FBD method is unpredictable even for anticipated seismic event. Further, cost of repairing structural damage is considerably higher and hence, in 1990s need of design method based on performance of building has been proposed in *Vision 2000* (SEACO 1995). Various researchers started working on development of new design approach which can handle the seismic design uncertainties in more rational way (Menon *et al.* 2018). Primarily, two categories of performance-based design approach are proposed in literature i.e. displacement based and energy based.

Generally, damage to the structure can be assessed in terms of strains developed in structural members. This strain can be computed in terms of displacement provided the geometry of structure is known (Vidot-Vega and Kowalsky 2010). During a seismic event, structures will undergo large inelastic displacements. Therefore, inelastic displacement considerations in seismic design is more rational (Priestley *et al.* 2007). Hence the displacement-based approaches states that, by controlling the relative displacement/drift of the structure, structural as well as non-structural damage can be controlled. Many researchers (Moehle 1992, Kowalsky *et al.* 1995, Priestley and Kowalsky 2000, Medhekar and Kennedy 2000, Pettinga and Priestley 2005, Priestley *et al.* 2007, Moghim and Saadatpour 2008, Massena *et al.* 2010, Dzakic *et al.* 2012, Fakhraddini and Salajegheh 2012, Muljati *et al.* 2015) worked on displacement based procedure to obtain realistic approximation of base shear and its distribution for RC bridges and building frames. To predict the inelastic displacement of structure Moehle (1992) proposed an iterative procedure which calculates the displacement demand and capacity of structure based on strength and stiffness of structure using displacement spectra. This procedure is iterative procedure in which strength and stiffness of structure are variables. Therefore, Kowalsky *et al.* (1995) proposed a direct displacement based method for ‘SDOF’ system like single pier RC bridge system of known mass to predict required stiffness of structure for desired displacement, based on correlation between displacement ductility, effective damping and displacement spectra (for respective effective damping). Further, Priestley and Kowalsky (2000) adopted same approach for multi degree of freedom system. In the design procedure proposed by Priestley *et al.* (2007) design storey displacements of RC frame building is calculated using normalized inelastic mode shape and the displacement of critical storey. Two different expressions have been proposed to predict normalized inelastic mode shape i.e., linear profile for building up to four storey and parabolic profile for taller buildings which is based on dynamic behaviour of RC frames (Loeding *et al.* 1998). The procedure makes use of substitute SDOF system instead of actual MDOF system

using design storey displacements (Medhekar and Kennedy 2000).

Second type of performance-based approach proposes that earthquake primarily transfers energy to structure and it will be more effective to design them for dissipating the input energy. However, during earthquake all the input energy transferred to the structure does not contribute to structural damage. A part of input energy gets dissipated through elastic deformations and rest by plastic deformations. Therefore, Housner (1956) proposed energy equation in a simple form along with limit state design. He used the difference between the input energy and elastic energy to obtain the plastic energy to be dissipated by the structure. However, later it has been identified that not all the input energy contributes to structural damage and a part of it gets dissipated by inherent damping of the structure. Hence, input energy modification factor (λ) has been introduced to incorporate the effect of inherent damping and which depend on the damping ratio, ductility and cumulative ductility factor (Kuwamura and Galambos 1989). Various researchers (Akiyama 1985, Kuwamura and Galambos 1989, Fajfar and Vidic 1994, Benevent-Climent *et al.* 2002) proposed different formulation to estimate input energy modification factor. Plastic energy dissipation directly depends on number and location of plastic hinge formation during seismic event. Generally, structures when subjected to severe earthquake shaking have many potential failure mechanisms, such as local mechanism, soft-story mechanism and global mechanism. Local failure and soft-story mechanisms require large ductility demand on components. Global failure mechanisms i.e., the strong-column weak beam mechanism can provide higher total energy dissipation with less ductility demand on components, which results in a more uniform story drift and better structural performance. Later, Leelataviwat *et al.* (1999) proposed a relatively new Performance-Based Plastic Design (PBSD) procedure using aforementioned energy balance equation for steel moment frames for the pre-selected mechanism and ultimate target drift. Further, Goel *et al.* (2010) revised the PBSD method for Reinforced Concrete (RC) moment frames and also introduced an energy modification factor (γ) to consider the energy component dissipated by the inherent damping. The basic energy balance equation was derived by assuming ideal elasto-plastic force-deformation behavior and full hysteretic loops for the system. This assumption may be valid for the ductile steel framing system, but RC elements does not possess such hysteretic property and hence shall be modified using appropriate factors. It can be applied in two ways viz. 1. Energy modified by a factor η to account for the reduced area of typical hysteretic loops as a fraction of the corresponding full loops, 2. The second is based on considering effect of degrading hysteretic behavior on peak displacement i.e., using factor C_2 given in FEMA 440 (2005). The Plastic Energy modification factor (η_p) depends on hysteretic damping component (ζ_H). Various researchers have proposed different formulation for computing hysteretic damping component (Gulkan and Sozen 1974, Kowalsky 1994, Priestley 2003, Dwairi *et al.* 2007). After detailed comparative study of various hysteretic damping

formulation and input energy modification factor Merter and Ucar (2017) concluded that, the hysteretic damping formulation suggested by Gulkan and Sozen (1974) and input energy modification factor proposed by Benavent-Climent *et al.* (2002) gives appropriate results in derivation of base shear using energy-based approach. Also, a comparative study of EBD approach with various hysteretic damping formulation and input energy factor proposed by various researcher have been conducted by Sivraj *et al.* (2018). Based on aforementioned research formulations proposed by Gulkan and Sozen (1974) and Benavent-Climent *et al.* (2002) have been used in calculation of energy-based base shear in present study.

These performance based methods (DDBD and EBD) consider inelastic seismic performance for designing structures and hence a rational prediction of structural behaviour can be achieved. In Direct Displacement Based Design (DDBD) approach the structure is designed to achieve a specified inelastic drift corresponding to the desired performance level. In Energy Based Design (EBD) approach, the structure is designed in order to achieve a specified performance level, defined by drift limit and corresponding energy dissipation. The design philosophy of aforementioned three design approaches is entirely different from each other for same seismic hazard. Further, nonlinear seismic performance of same structure designed using these three approach will be different. Therefore, objective of the present work is to investigate advantage and limitation of each considered approaches by studying FBD, DDBD and EBD procedure, and non-linear performance of a six storey RC frame designed using these approaches.

2. Design procedures

The FBD, DDBD and EBD are three conceptually different design approaches therefore, it is difficult to directly compare the strength, stiffness and ductility properties of structure designed by these methods. To compare these three approaches, inelastic design drift can be considered as the primary criteria for structural design. Therefore, an attempt has been made to compare the design base shear, lateral force distribution, design procedure and nonlinear performance of a selected frame designed using these approaches for the 2 percent design drift. A brief description of the three design approaches are presented in following sections.

2.1 Force based design procedure

In force based seismic design procedure the stiffness of members is estimated from preliminary member sizes and accordingly the fundamental modal periods are estimated. It is to be noted that, most of the design codes provide capping of period, therefore, the design lateral forces calculated from stiffness-based period are not allowed to fall below the lateral force estimated using empirical 'height dependent' period formula. Indian standard IS 1893(1):2016 code specifies a height (h) dependent fundamental period (T_a) expressions (Eq. (1)).

$$T_a = 0.075h^{0.75} \text{ (for bare RC moment resisting frame)} \quad (1)$$

Further, the design horizontal seismic coefficient A_h for the structure shall be determined using Eq. (2).

$$A_h = \frac{\left(\frac{Z}{2}\right)\left(\frac{S_a}{g}\right)}{\left(\frac{R}{I}\right)} \quad (2)$$

Where, Z is the seismic zone factor provided in IS 1893(1):2016 based on the seismic intensity, I is an importance factor reflecting different level of acceptable risk based on the type of structure, R is the force reduction factor based on lateral load resisting system and (S_a/g) is design acceleration coefficient for different soil types, normalized with peak ground acceleration, corresponding to natural period of structure. The design base shear V_b along any principal direction of a building is calculated using the horizontal seismic coefficient (A_h) and seismic weight of the structure (W) (Eq. (3)).

$$V_b = A_h W \quad (3)$$

This design base shear at base level is distributed over the height of structure and internal force distribution at member level is determined from the analysis.

2.2 Direct displacement based design procedure

In DDBD, the structure is designed using equivalent Single-Degree-of-Freedom (SDOF) representation of the real structure considering desired inelastic displacement response, rather than by its initial elastic characteristics (Fig. 1). In FBD, elastic (pre-yield) properties like initial stiffness ' K_i ' & elastic damping are used. Whereas, DDBD characterizes the structure by secant stiffness ' K_e ' at maximum displacement ' Δ_d ' and equivalent viscous damping representative of combined elastic damping and hysteretic energy absorbed during inelastic response. The characteristic design displacement (Δ_d) of the substitute structure (SDOF) depends on the limit state deformation of the most critical member of the real structure, and target displacement profile of the structure. Even though the design steps for DDBD suggested by several researchers (Dzagic *et al.* 2012, Fakhreddini and Salajegheh 2012, Moghim and Saadatpour 2008, Pettinga and Priestley 2005, Priestley *et al.* 2007, Priestley and Kowalsky 2000) are similar, yet they differ in terms of consideration of various parameters such as target displacement profile, equivalent viscous damping equation and the base shear distribution pattern in the design process. The DDBD formulation prescribed by Priestley *et al.* (2007) has been used in the present study and relevant equations are summarised. In the first stage multi degree of freedom (MDOF) system (i.e., frame) is represented with equivalent SDOF (Fig. 1) using Eqs. (4) and (5)

$$H_e = \frac{\sum_{i=1}^n (m_i \Delta_i H_i)}{\sum_{i=1}^n (m_i \Delta_i)} \quad (4)$$

$$m_e = \frac{\sum m_i \Delta_i}{\Delta_d} \quad (5)$$

The normalized inelastic mode shape ' δ_i ' of the MDOF frame structure obtained using relationship between the height of storey ' H_i ' and total height structure ' H_n ', based on number of stories ' n ' (Eq. (6)).

$$\begin{aligned} \text{for } n \leq 4: \delta_i &= \frac{H_i}{H_n} \\ \text{for } n > 4: \delta_i &= \frac{4}{3} \left(\frac{H_i}{H_n} \right) \left(1 - \frac{H_i}{4H_n} \right) \end{aligned} \quad (6)$$

The design storey displacements ' Δ_i ', are calculated using the shape vector ' δ_i ' scaled with respect to the critical storey displacement ' Δ_c ' and to the corresponding mode shape at the critical storey level ' δ_c ' (Eq. (7)).

$$\Delta_i = \delta_i \left(\frac{\Delta_c}{\delta_c} \right) \quad (7)$$

The equivalent design displacement ' Δ_d ' is to be derived from those of the MDOF system by the relationship (Eq. (8))

$$\Delta_d = \frac{\sum_{i=1}^n (m_i \Delta_i^2)}{\sum_{i=1}^n (m_i \Delta_i)} \quad (8)$$

Where, ' m_i ' and ' Δ_i ' are the masses and displacements of the n^{th} significant mass locations respectively. Various studies (like Dwairi *et al.* 2007) provides relationship for conservative estimation of equivalent viscous damping based on ductility (Fig. 2). Hence, to determine equivalent viscous damping, ductility (μ) of equivalent SDOF system has been determined based on its design displacement ' Δ_d ' and yield displacement ' Δ_y ' (Eq. (9)).

$$\mu = \Delta_d / \Delta_y \quad (9)$$

The effective period of equivalent SDOF system ' T_e ' at maximum displacement response measured at the effective height ' H_e ' can be read from a set of displacement spectra for different levels of damping, as shown in Fig. 3.

The effective stiffness ' K_e ' of the equivalent SDOF system at maximum displacement is thus obtained by Eq. (10).

$$K_e = 4 \pi^2 m_e / T_e^2 \quad (10)$$

The design base shear force, ' F ' is consequently can be estimated based on ' K_e ' and ' Δ_d ' of substitute structure (Eq. (11))

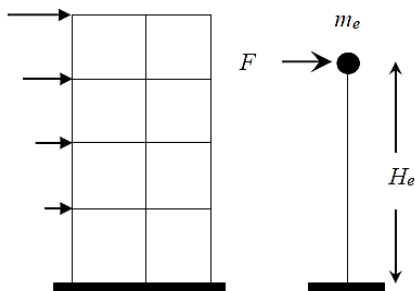


Fig. 1 Equivalent SDOF representation of building

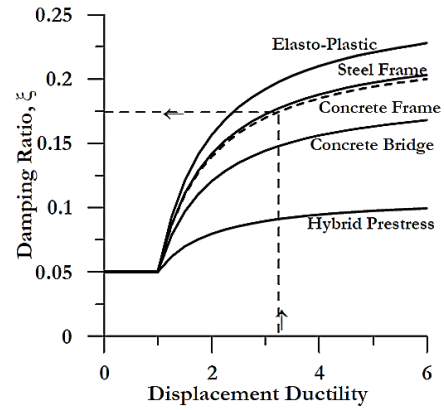


Fig. 2 Equivalent viscous damping vs. ductility

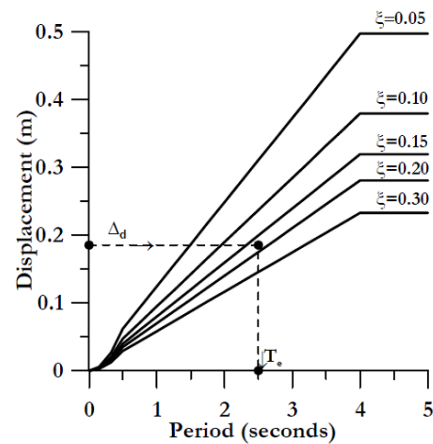


Fig. 3 Design displacement spectra

$$F = V_{Base} = K_e \Delta_d \quad (11)$$

2.3 Energy based design procedure

Housner (1956) proposed use of energy equation in a simple form along with limit states for designing structures. In the proposed method, difference between input energy and elastic energy has been used to obtain the plastic energy, which is required to be dissipated by structure through plastic actions (Eq. (12)).

$$E_e + E_\xi + E_p = E_I \quad (12)$$

Where, ' E_e ' is elastic vibrational energy, ' E_ξ ' is the energy absorption due to miscellaneous damping, ' E_p ' is the inelastic strain energy required to be dissipated by structure and ' E_I ' is the earthquake input energy (Akiyama 1988). Maximum earthquake input energy for a multi-degree-of-freedom system has been estimated using kinetic energy formulation considering first fundamental mode of vibration (Eq. (13))

$$E_I = \frac{1}{2} M S_v^2 = \frac{W g a^2 T^2}{8 \pi^2} \quad (13)$$

Where, ' M ' is total mass of the system, ' S_v ' is pseudo-velocity from the elastic response spectrum, ' a ' is normalized pseudo-acceleration with respect to ' g ', ' W ' is

total seismic weight of building; and ' T ' is fundamental natural period of structure. Kato and Akiyama (1982) and Akiyama (1985) shown that, elastic energy ' E_e ' can be estimated with a reasonable accuracy by assuming that the entire structure is reduced into an equivalent single-degree-of-freedom system as

$$E_e = \frac{1}{2} M \left(\frac{T}{2\pi} \cdot \frac{V_y}{W} \cdot g \right)^2 \quad (14)$$

Where, ' V_y ' is the yield base shear.

All the input energy contributes to structural damage and inherent damping of the structure dissipates a part of it. Hence, input energy modification factor (λ) is introduced to incorporate the effect of inherent damping and is dependent on the damping ratio, ductility and cumulative ductility factor (Kuwamura and Galambos 1989). The energy Eq. (12) is modified with plastic energy modification factor (η) and input energy modification factor (λ), which is acceptable for all structural systems.

$$E_e + \eta_p \cdot E_p = \lambda \cdot E_I \quad (15)$$

The Plastic Energy modification factor ' η_p ' depends on hysteretic damping component ' ζ_H '. Various researchers have proposed different formulation for computing hysteretic damping component ' ζ_H ' and input energy modification factor ' λ '. Based on the work-energy principal, Merter and Ucar (2017) obtained energy based yield base shear by equating plastic energy of MDOF system to the external work done by the equivalent inertia force considering the plastic energy equation is in terms of ' η_p ' and ' λ ' factors as,

$$\frac{\lambda}{\eta_p} \cdot \sum_{n=1}^N E_{I(SDOF)n} \Gamma_n^2 - \frac{1}{2} \cdot \frac{M}{\eta_p} \left[\frac{T}{2\pi} \cdot \frac{V_y}{W} \cdot g \right]^2 = V_y \cdot \theta_p \cdot \left[\frac{\sum_{i=1}^n w_i h_i^2}{\sum_{j=1}^n w_j h_j} \right] \quad (16)$$

Where, ' Γ_n ' is the modal participation factor of the n^{th} mode, ' $E_{I(SDOF)n}$ ' is input energy of an equivalent a SDOF system with vibration properties of the n^{th} mode of MDOF system, ' θ_p ' is the plastic drift of the structure, ' w_i ' is the seismic weight of i^{th} floor and ' h_i ' is the height of storey level from ground.

3. Specification of building

A six storey RC bare frame building has been considered which represents a mid-rise building (Fig. 4) as per model building types of HAZUS (2006). A constant storey height of 3 m is considered for all floors. The building is assumed to be situated on stiff soil and located in the highest seismic zone of India i.e., zone V with peak ground acceleration as 0.36g as per IS 1893 (1):2016. Frame is designed as special moment resisting frame (SMRF) with response reduction factor as 5. The reinforced concrete frames are made using concrete with nominal characteristic compressive strength of 30 MPa (M30) and the reinforcing steel having yield strength of 415 MPa (HYSD 415). The reinforced concrete slab thickness at each floor level is assumed as 150 mm. In the design of building

gravity loads viz. self-weight (considering unit weight of reinforced concrete as 25 kN/m³), 3 kN/m² live load and 1 kN/m² floor finish load have been considered.

Effective stiffness of elements as per Kumar and Singh (2010) has been used in modelling. As explained earlier, in FBD as per IS 1893 (1): 2016 the elastic deflection calculated for un-factored lateral load and checked for inter-storey drift limit to remain within 0.004. IS 1893 (1): 2016 code approximates maximum inelastic displacement of building ' R ' times its elastic displacement in calculation of separation gap. Hence, the maximum inelastic inter storey drift can be approximated as ' R ' time elastic drift 0.4% i.e. 2%. Therefore, the considered building frame (as shown in Fig. 4) has been designed using DDBD and EBD for 2% design drift. The design philosophy of all three procedures is distinct from each other and considers different design parameters in design procedure. Various design parameters and design base shear of FBD, DDBD and EBD for considered building frame are summarised in Table 1.

Further, the design base shear has been distributed over the height to determine internal force distribution and design forces for structural members.

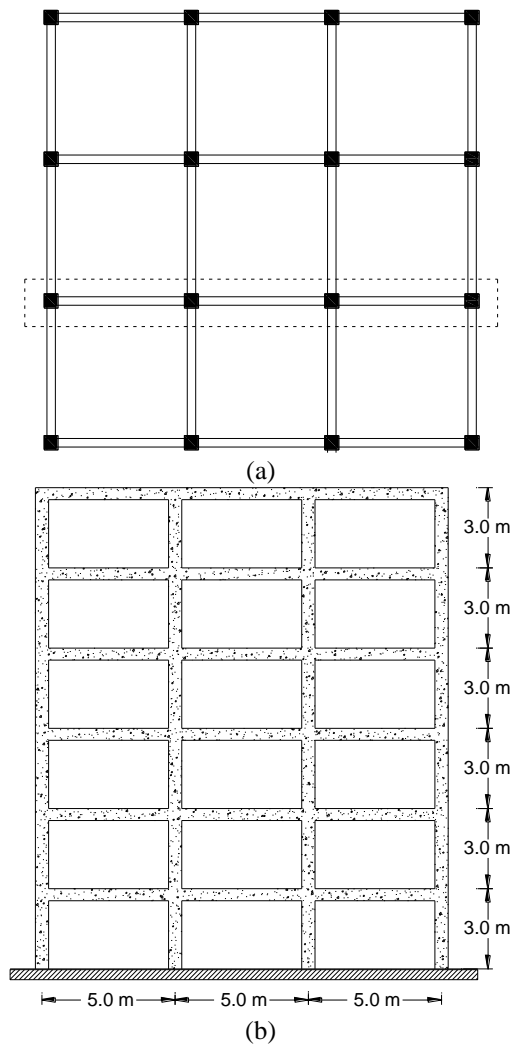


Fig. 4 (a) Floor plan of building and (b) Elevation of six storey RC moment resisting frame

Table 1 Design parameters of FBD, DDBD and EBD approach

FBD parameters								
Z	I	R	T (sec.)	Sa/g	A _h	Design Base Shear (kN)		
0.36	1	5	0.66	2.08	0.075	255		
DDBD parameters								
Δ _d (m)	m _e (kg)	H _e (m)	μ	ξ (%)	R	T _e (sec.)	K _e (kN/m)	Design Base Shear (kN)
0.21	378050	12.66	1.32	9.35	0.83	2.08	3434	727
EBD parameters								
λ	η _p	Mode 1 E _{I(SDOF)} .Γ _n ²	Mode 2 E _{I(SDOF)} .Γ _n ²	Mode 3 E _{I(SDOF)} .Γ _n ²	Design Base Shear (kN)			
0.261	0.180	103996.9	5328.6	405.8	983			

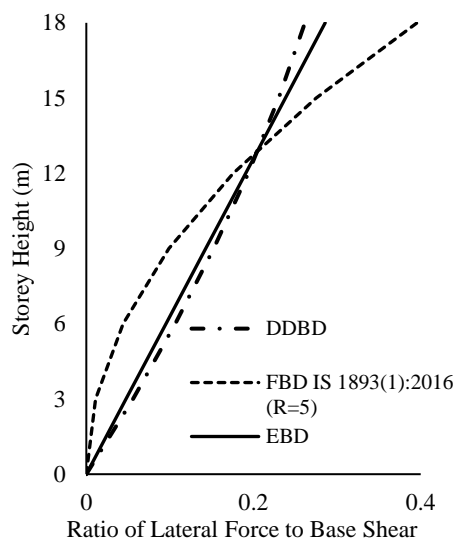


Fig. 5 Comparative plot of FBD, DDBD and EBD base shear force distribution

3.1 Lateral force distribution

Later force distribution pattern significantly affects the force distribution in various elements of the building. The design base shear distribution given in the seismic design codes (i.e., for FBD) are typically based on results of elastic-response studies (Chao *et al.* 2007). In DDBD approach the base shear force is distributed to storey levels in proportion to the product of the storey mass and the storey displacement (Priestly *et al.* 2007). In this approach the storey displacements are estimated using normalized inelastic mode shape and design displacement at critical storey level. EBD approach considers global failure mechanism of frame and adopt linear distribution of base shear over the height due to formation of mechanism (Goel *et al.* 2010). Fig. 5 shows the normalized lateral force (i.e., ratio of lateral force to base shear) variation along storey height for the three considered approaches. FBD procedure in IS 1893(1): 2016 code considers a parabolic force distribution pattern (it is to be noted that different national codes consider different force distribution pattern). Some

EBD approaches (like Akiyama 1988) don't considers linear variation of storey forces along height, however by assuming global hinge formation in the frame inverted triangular force distribution along the height structures has been considered in present study (Leelataviwate *et al.* 1999 and Goel *et al.* 2010). The force distribution pattern in DDBD approach depends on number of storeys i.e. linear pattern for buildings up to four storeys and parabolic pattern for taller buildings. In present study the force distribution pattern in DDBD approach proposed by Priestley *et al.* (2007) has been used.

3.2 Structural design of RC elements

Using base shear calculations by each of the three approaches i.e. FBD, DDBD and EBD, proportioning of the section sizes and reinforcement in the structural members have been apportioned. The preliminary section sizes of beams and columns have been selected using minimum dimensions provided in ductile detailing code (IS 13920:2016) and serviceability criteria suggested in IS 456:2000. Limit state design procedure has been used for designing the members. To attend desired global mechanism of frame under seismic loading, the FBD approach recommends special ductility provisions (i.e., IS 1893(1): 2016 recommends IS 13920:2016 provisions for ductile design and detailing), DDBD approach proposes capacity design approach (Priestly *et al.* 2007) and EBD approach follows plastic design method modified by Goel *et al.* (2010), Bai and Ou (2012) as column tree method. The column size has been proportioned by limiting the column reinforcement to maximum of 3 percent. Further, in FBD frame, it has been ensured that at any beam-column joint the sum of column design strength will be 1.4 times more than that of sum of beam design strength. In the present study while fixing the beam dimensions, number of analysis and design trials has been performed with different depth of beam for all three approaches and possible beam dimensions have been identified. However, the yield rotation capacity of beam primarily depends on its depth (Priestley *et al.* 2007) and plays significant role in estimating seismic demand in case of DDBD and EBD approach. Therefore, to maintain the uniformity in yield

Table 2 Details of frame members and reinforcement designed as per (a) FBD, (b) DDBD and (c) EBD approach

Approach	Floor Level	Beam			Column	
		Dimension (mm)	Reinforcement		Dimension (mm)	Reinforcement
			Top	Bottom		
FBD	1 st Floor	300 x 450	3 No. 20 mm ϕ + 2 No. 16 mm ϕ	3 No. 20 mm ϕ	450 x 450	16 No. 20 mm ϕ
	2 nd Floor	300 x 450	4 No. 20 mm ϕ + 2 No. 16 mm ϕ	2 No. 20 mm ϕ + 2 No. 16 mm ϕ	450 x 450	16 No. 20 mm ϕ
	3 rd Floor	300 x 450	4 No. 20 mm ϕ + 2 No. 16 mm ϕ	2 No. 20 mm ϕ + 2 No. 16 mm ϕ	450 x 450	16 No. 20 mm ϕ
	4 th Floor	300 x 450	3 No. 20 mm ϕ + 2 No. 16 mm ϕ	3 No. 20 mm ϕ	450 x 450	16 No. 16 mm ϕ
	5 th Floor	300 x 450	2 No. 20 mm ϕ + 2 No. 16 mm ϕ	2 No. 16 mm ϕ + 1 No. 12 mm ϕ	450 x 450	16 No. 16 mm ϕ
	6 th Floor	300 x 450	2 No. 20 mm ϕ + 2 No. 16 mm ϕ	2 No. 16 mm ϕ + 1 No. 12 mm ϕ	450 x 450	16 No. 16 mm ϕ
DDBD	1 st Floor	300 x 450	7 No. 20 mm ϕ	4 No. 20 mm ϕ + 1 No. 16 mm ϕ	500 x 500	16 No. 20 mm ϕ
	2 nd Floor	300 x 450	7 No. 20 mm ϕ	4 No. 20 mm ϕ + 1 No. 16 mm ϕ	500 x 500	16 No. 20 mm ϕ
	3 rd Floor	300 x 450	4 No. 20 mm ϕ + 3 No. 16 mm ϕ	3 No. 20 mm ϕ + 1 No. 16 mm ϕ	500 x 500	16 No. 20 mm ϕ
	4 th Floor	300 x 450	4 No. 20 mm ϕ + 1 No. 16 mm ϕ	2 No. 20 mm ϕ + 1 No. 16 mm ϕ	500 x 500	12 No. 20 mm ϕ + 4 No. 12 mm ϕ
	5 th Floor	300 x 450	3 No. 20 mm ϕ + 2 No. 12 mm ϕ	2 No. 20 mm ϕ	500 x 500	12 No. 20 mm ϕ + 4 No. 12 mm ϕ
	6 th Floor	300 x 450	3 No. 20 mm ϕ + 2 No. 12 mm ϕ	2 No. 20 mm ϕ	500 x 500	12 No. 20 mm ϕ + 4 No. 12 mm ϕ
EBD	1 st Floor	300 x 450	7 No. 20 mm ϕ	3 No. 20 mm ϕ + 3 No. 16 mm ϕ	550 x 550	24 No. 22 mm ϕ
	2 nd Floor	300 x 450	7 No. 22 mm ϕ	5 No. 20 mm ϕ + 2 No. 16 mm ϕ	550 x 550	24 No. 22 mm ϕ
	3 rd Floor	300 x 450	4 No. 22 mm ϕ + 3 No. 16 mm ϕ	3 No. 22 mm ϕ + 2 No. 16 mm ϕ	550 x 550	24 No. 22 mm ϕ
	4 th Floor	300 x 450	5 No. 20 mm ϕ + 2 No. 16 mm ϕ	4 No. 20 mm ϕ	550 x 550	24 No. 22 mm ϕ
	5 th Floor	300 x 450	4 No. 20 mm ϕ + 1 No. 16 mm ϕ	2 No. 20 mm ϕ + 1 No. 16 mm ϕ	550 x 550	24 No. 22 mm ϕ
	6 th Floor	300 x 450	4 No. 20 mm ϕ + 1 No. 16 mm ϕ	2 No. 20 mm ϕ + 1 No. 16 mm ϕ	550 x 550	24 No. 22 mm ϕ

Φ - diameter of reinforcing bar

rotation, optimum beam depth of 450 mm has been considered in all the three methods.

In all the three approaches it has to be ensured that a shear failure does not precede the actual yielding of the beam in flexure. Therefore, in the present study transverse reinforcement design at potential hinge location for all three approaches has been done as per the provisions of IS 13920:2016 and IS 456:2000. In case of beam, capacity shear i.e., the design shear force due to formation of plastic hinges at both ends of the beam plus the factored gravity shear force on the span has been considered. Similarly, in case of column, higher of the calculated shear force as per analysis and the shear force due to plastic hinge formation in beam has been considered for design. In shear design, the shear capacity of concrete has been ignored and only dependent on shear reinforcement. Based on the assessment, 2 legged stirrups of 10 mm diameter reinforcing bar at 100 mm spacing and 4 legged stirrups of

10 mm diameter reinforcing bar at 100 mm spacing has been provided in all beams and column, respectively. Details of storey frame properties and reinforcement designed as FBD, DDBD and EBD is given in Table 2.

Further, performance of all three frames has been assessed using nonlinear static analysis (i.e. pushover) and nonlinear dynamic analysis (i.e. nonlinear time history analysis). Lumped plastic hinge model as per ASCE 41-17 has been used to simulate the nonlinear behavior of members. In case of beam members, uncoupled moment hinges (M3 hinge) and for column members, coupled axial force and uniaxial bending moment hinges (P-M2 hinge), have been assigned at both the ends. Takeda Hysteresis model has been used for simulating the degrading hysteretic behaviour of reinforced concrete in nonlinear analysis (Takeda *et al.* 1970). Analysis has been performed using structural analysis software SAP2000 version 20.

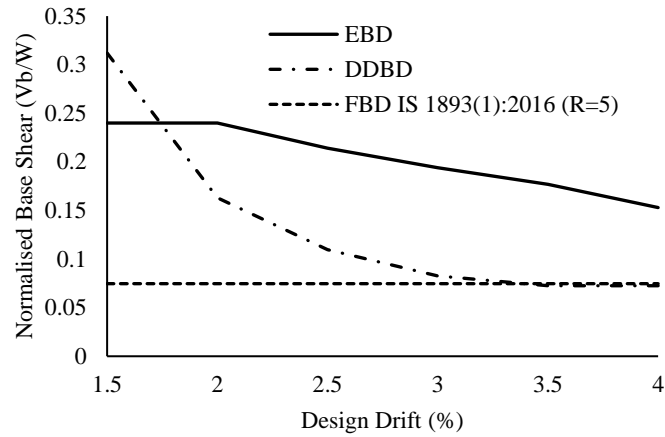


Fig. 6 Plot of normalized base shear vs percentage design drift as per FBD, DDBD and EBD approach

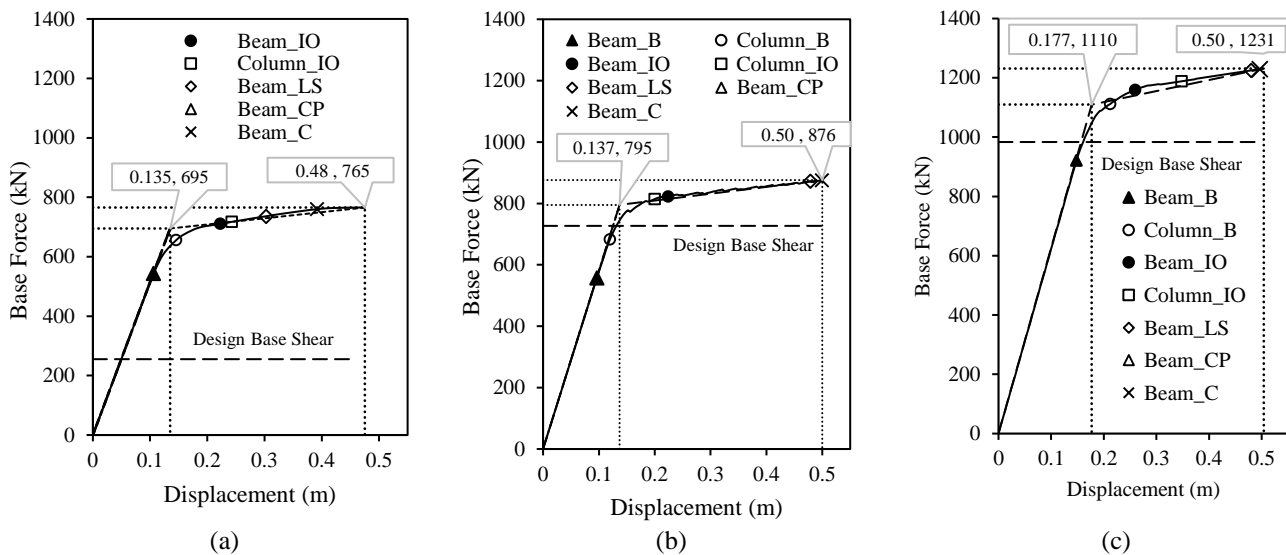


Fig. 7 Capacity curves of the frame designed using (a) FBD, (b) DDBD and (c) EBD approach

4. Design base shear

In FBD procedure reduced elastic base shear is used for designing the buildings. The reduction of elastic base shear depends on expected ductility and over strength, which can be achieved by structural design and detailing. Generally, two response reduction factors viz. 3 and 5 for ordinary RC moment resisting frame and special RC moment resisting frame, respectively, is suggested in IS 1893 Part 1 (2016). It is to note that in FBD method, design base shear is independent of drift. Whereas, in both DDBD and EBD procedure design base shear depends on the design drift for the anticipated level of earthquake and expected performance. In present study five design drift limit ' θ_d ' values (i.e. inelastic drifts) from 1.5 percent to 3.5 percent (with increment of 0.5 percent) have been considered for the selected building and corresponding design base shear ' V_b ' has been obtained using both DDBD and EBD approach. In DDBD and EBD approach ductility demand of structure is correlated with design drift and gross estimate of yield rotation capacity of beams.

For the considered frame (as discussed in previous section) a comparison of variation of normalized base shear with design drift for DDBD and EBD approach has been plotted (Fig. 6). Additionally, the reduced design base shears for ' R ' as 3 and 5 has also been plotted. While design base shear falls below the FBD design base shear (for ' R ' as 5). In EBD approach the base shear is estimated using amount of the input energy dissipated through elastic and plastic actions. As plastic deformations are relatively very less for low design drifts the structure shall be capable of dissipating large part of input energy through elastic action only, therefore, EBD approach also estimates higher design base shear in low drift range. It is to note that as the value of design drift limit increases, the ductility demand of structure increases leading to more damping in structure and thereby, resulting in reduction of design base shear. Similar trend of seismic demand can be observed from Fig. 6 for both the DDBD and EBD approach at different discrete drift levels.

Table 3 Capacity curve results

Approach	Time Period (s)	Ratio of Elastic FBD base shear to yield base shear	Target Displacement (m)	Ratio of Target Displacement to Yield Displacement	Initial stiffness (kN/m)
FBD	1.296	1.8	0.224	1.660	5148
DDBD	1.275	1.6	0.220	1.605	5802
EBD	1.171	1.1	0.202	1.141	6271

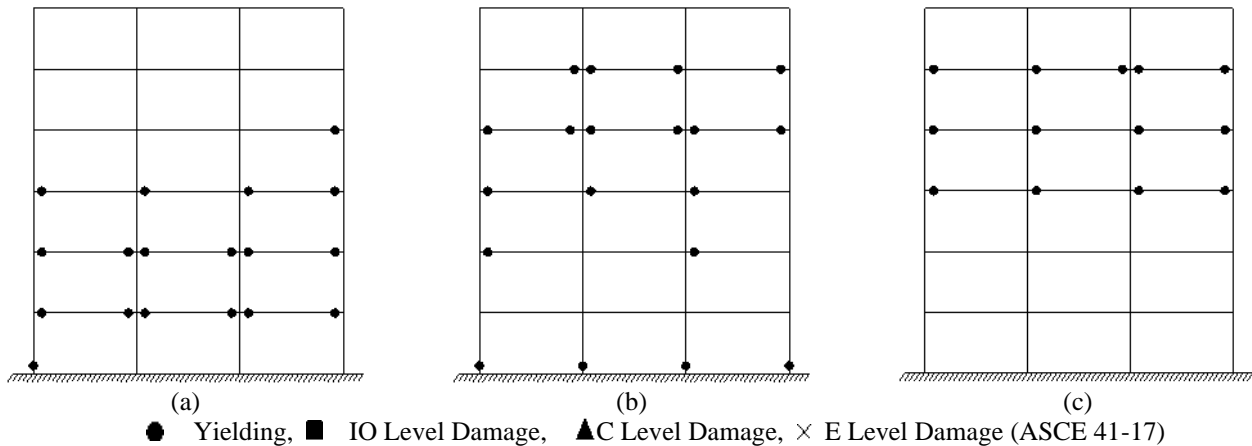


Fig. 8 Plastic hinge formation in (a) FBD, (b) DDBD and (c) EBD frame at global yielding state

5. Nonlinear static analysis results

Nonlinear static analysis (ATC-40, 1996) i.e., Pushover analysis has been performed on the frames designed using the three approaches. Fig. 7(a) to 7(c) shows the capacity curves (force-displacement curve) with different damage levels in beams and columns for FBD, DDBD and EBD frames, respectively. This curve has been bi-linearized as per the procedure prescribed in ASCE 41-17. Based on the idealized force-displacement curve initial stiffness, target displacement and ratio of target displacement to yield displacement of the frames have been calculated and summarised in Table 3. The difference in fundamental natural period of the three frames shown in table indicates that in comparison to DDBD and EBD approaches the frame designed using FBD approach leads to relatively flexible structure, which is also reflected from the difference in initial stiffness (i.e., initial stiffness of DDBD and EBD frame is 1.13 and 1.2 times more than FBD frame, respectively). Ratio of elastic FBD base shear to yield base shear and ratio of target displacement to yield displacement shows that strength and ductility properties of FBD and DDBD frame are very similar. For assessment of the weak links in the frame designed as per FBD, DDBD and EBD plastic hinge formation pattern under monotonic loading has been compared in Fig. 8 at global yielding (i.e., at yield point of idealized capacity curve, marked in Fig. 7) and in Fig. 9 for ultimate base shear level (marked in Fig. 7).

At global yielding state, effective yielding (B Level) have been observed in few members (viz. beam and column) but at different locations in the frames designed using three approaches. In FBD frame effective yielding started in bottom storey beams and at one bottom of column which is subject to reduced axial load due to lateral loading

(Fig. 8(a)). On the other hand, in DDBD and EBD frame effective yielding started in beams at upper storeys only (Figs. 8(b) and 8(c)). However, at ultimate base shear collapse level damage has been observed in all the three frames. In case of FBD frame, strong column weak beam concept has been followed by providing strength differential of 1.4 times, still unintended hinges have been observed in columns at intermediate storey level (Fig. 9(a)). This frame (Figs. 9(b) and 9(c)). Both the approaches confirm strong column weak beam design, however, the column tree method for the EBD frame requires relatively large column sections and more reinforcement than the DDBD.

6. Nonlinear time history analysis

Nonlinear static analysis in the previous section has elaborated the inherent capacity and general behaviour of the frame designed using three approaches, however, to understand the actual seismic behaviour nonlinear time history analysis has been performed for suit of ten real ground motion time history. It is well known that the ground motion records used for the time-history analysis significantly influences the structural response. In the following section the selection procedure of ground motion adopted in present study has been explained.

6.1 Selection of ground motion records

The time-history analysis can be performed using artificial accelerograms and recorded or simulated accelerograms (EN 1998-1:2004, 2004). The artificial accelerograms are generated from a computer based algorithms, which are used 1) to generate a power spectral

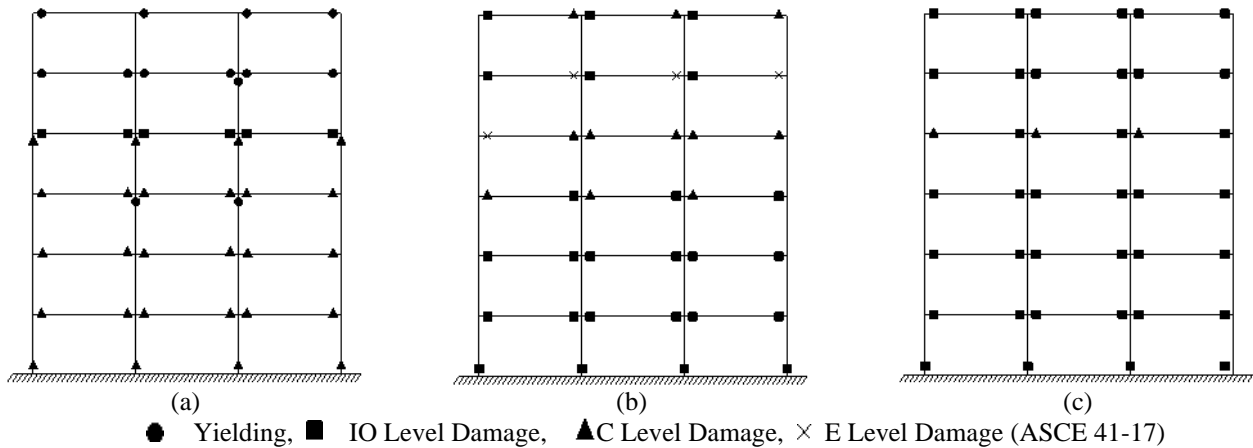


Fig. 9 Plastic hinge formation in (a) FBD, (b) DDBD and (c) EBD frame at ultimate base shear

Table 4 Details of selected ground motions for nonlinear time history analysis

RSN*	Event Name	Recording Station	Year	$V_{s,30}$ ^a (m/s)	EC-8 Site Class	M_w ^b	R_{jb} ^c
169	Imperial Valley-06	Delta	1979	242.05	C	6.53	22.03
725	Superstition Hills-02	Poe Road (temp)	1987	316.64	C	6.54	11.16
778	Loma Prieta	Hollister Differential Array	1989	215.54	C	6.93	24.52
987	Northridge-01	LA - Centinela St	1994	321.91	C	6.69	20.36
1077	Northridge-01	Santa Monica City Hall	1994	336.2	C	6.69	17.28
1203	Chi-Chi_Taiwan	CHY036	1999	233.14	C	7.62	16.04
5780	Iwate_Japan	Iwadeyama	2008	345.55	C	6.9	20.77
5823	El Mayor-Cucapah_Mexico	Chihuahua	2010	242.05	C	7.2	18.21
6923	Darfield_New Zealand	Kaipoi North School	2010	255	C	7	30.53
5975	El Mayor-Cucapah_Mexico	Calexico Fire Station	2010	231.23	C	7.2	19.12

Records were selected from the Pacific Earthquake Engineering Research Center Next Generation of Ground motion Attenuation Models West 2 database.

* Record Sequence Number

^a Average shear-wave velocity of the upper 30 m of soil.

^b Moment magnitude M_w .

^c Joyner-Boore distance in km (closest horizontal distance to the surface projection of the rupture plane).

density function from code based response spectrum and 2) to iteratively modify sinusoidal signals derived from it till the response matches with the target response spectra (Bommer and Acevedo 2004). The simulated accelerograms are obtained from point source stochastic simulations through their extension to finite sources to dynamic model of rupture and by accounting the path and site effects (Boore 2003). However, various studies (Araújo *et al.* 2016, Bommer and Acevedo 2004; Iervolino and Cornell 2005, Iervolino *et al.* 2008) highlighted the uncertainties involved and state-of-art expertise required to use the aforementioned tools to derive precise artificial or simulated accelerograms.

In recent days, easy accessibility to extensive metadata of real ground-motion records is available (e.g., PEER NGA-West2 Database), thus promoting its use in response assessment of structures. Various national standards like Eurocode 8 (EC8-1), American Standard (ASCE-7) and New Zealand Standard (NZS 1170.5:2004) allow real ground-motion records for the analysis and provides the guidelines for their selection. However, selecting real

ground-motion records compatible to code based uniform response/hazard spectra becomes difficult due to its non-smoothed response spectra and significant variability in records. Bommer and Ruggeri (2002), highlighted that, recommendations provided in seismic design codes worldwide for the selection and scaling of ground motion records to be used in dynamic analyses are not sufficient. Therefore, various approaches like wavelet-based transform have been evolved to modify the real record in time or frequency domain to match the spectra with target code based spectra. In wavelet-based transform, real ground motion split into required number of time histories in non-overlapping frequency band and scaling them up or down iteratively such that response of complied time history will match the target spectra (Mukherjee and Gupta 2002). However, with reference to various studies Iervolino *et al.* (2008) highlighted that, spectral matching results in non-conservative response estimation. Due to spectral matching certain valuable aspects of earthquake can be lost which were inherently preserved by real ground motion record.

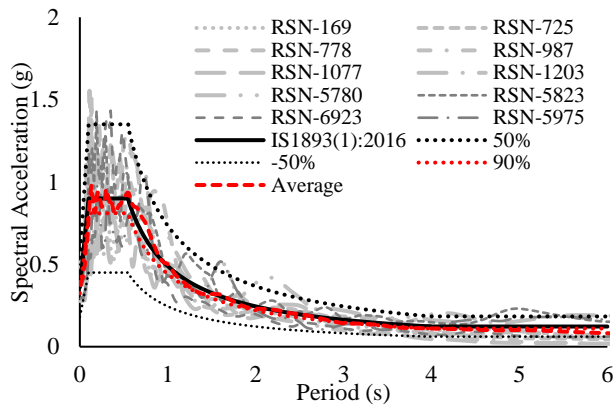


Fig. 10 Response spectra of the ten normalized time history record set, average spectra and IS 1893(1):2016 response spectra of zone V (PGA=0.36g) for medium soil

Therefore, in present study set of real ground motion records have been selected primarily based on EC-8 selection method along with some additional selection criteria's (Table 4 and Fig. 10). To obtain stable mean response ten real ground motions have been selected as suggested by Bommer and Acevedo (2004). To avoid potential event based bias in record sets maximum two records have been selected from one event (FEMA P695). Indian seismic code (part 1 of IS 1893:2016) classify the soil based on description of site class and standard penetration test (SPT) value. Therefore, approximate comparison of site classification of Indian seismic code with other national code is given by Adhikary and Singh (2012) and has been used in present study to correlate Indian seismic code specified site class to average seismic shear velocity (V_{S30}). The building is situated on medium soil (Type -II) of IS 1893:2016 classification, and the equivalent site class is C of EC-8 ($180 < V_{S30} < 360$ m/s) as per Adhikary and Singh (2012). Hence ground motion data recorded on the EC-8 site class C have been selected. Also, as Krawinkler *et al.* (2003) concluded that the frequency characteristics of ordinary ground motion within magnitude range of about 5.5 to 7 and recorded at distance more than 15 km from source are very less sensitive to magnitude and distance, therefore, in the present study most of the ground motion records are selected to meet these criteria with some exceptions. Selection and scaling has been done based on the EC8-1 criteria which suggest the average zero period acceleration values required to be higher than zero period acceleration value of code based spectra. To reduce the record to record variability, an additional criterion of imposing spectral mismatch limits relative to target IS 1893(1):2016 spectrum have been employed $\pm 50\%$ for each individual record as suggested by Araújo *et al.* 2016 (Fig. 10). Details of selected ground motion record is summarised in Table 4.

6.2 Nonlinear time history analysis result

Nonlinear time history analysis of the frames has been performed for all the ten selected ground motions (Table 4). Various studies (Dzagic *et al.* 2012, Goel *et al.* 2010,

Leelataviwat *et al.* 1999, Merter and Ucar 2017, Moghim and Saadatpour 2008, Priestley and Kowalsky 2000, Vidot-Vega and Kowalsky 2010) consider maximum interstory drift from nonlinear time history analysis as indicator of damage. Therefore, in present study, the comparative assessment of global as well as local damage has been done based on maximum interstory drift ratio. Bradley (2011) pointed out that, ground motion selection criteria's given by various codes and guidelines attempt to predict the mean seismic response from limited number of analysis without sound theoretical basis. Therefore, they proposed a rational probability based approach for determining the design seismic demand based on the analysis results. This method uses 84th percentile of the sample mean, therefore it takes account of i) the number of ground motion, ii) effect of ground motion selection and scaling, and iii) effect of spectral mismatch or variability. Araújo *et al.* (2016) also recommends application of this procedure in design and/or assessment using time history analysis. Nonlinear time history analysis results for design hazard level shows that, interstory drift (i.e. maximum response) of FBD, DDBD and EBD frame at all storey is well within the 2% drift limits. Fig. 11 shows the interstory drift demand of frames designed as per a) FBD, b) DDBD and c) EBD approach for design hazard level (i.e., PGA = 0.36 g).

The maximum value of 84th percentile of the sample mean interstory drift ratio ' $\delta_{0.84}$ ' is approximately same i.e., 1.33% in both FBD and EBD frame but at different storey level whereas; in case of DDBD frame it is relatively less i.e., 1.26%. Indian code IS 1893: 2016 Part 1, increases the calculated seismic design forces by a factor of 1.5 in design load combinations and therefore, in present study an elevated PGA level of 0.54 g has also been considered to assess the condition of frame at higher earthquake force. Therefore, to assess the performance for hazard higher than design level time history analysis has been performed by scaling up all time history to 1.5 time more PGA level and comparative maximum interstory drift ratio is shown in Fig. 12.

When all time histories scaled up by 50% then ' $\delta_{0.84}$ ' of FBD frame is 2.1% and exceeded the 2% drift limit. On the other hand, the maximum ' $\delta_{0.84}$ ' value of DDBD and EBD frame is 1.76% and 1.8%, respectively, and in well within the 2% drift limit. Significant difference in drift profile can be observed from comparative assessment of drift plots of FBD, DDBD and EBD frame (Figs. 11 and 12). Excessive drift in ground storey of FBD frame indicates excessive softness developed in bottom storey of frame due hinge formation in bottom storey columns. This effect has not been evidenced in other two design approach. Further, drift profile of DDBD frame has relatively uniform drift over the height and EBD frame has higher drift in middle storey.

Hysteretic energy is also an indicator in evaluating the seismic performance of structures. If no energy-dissipating device is used in a structure, high hysteretic energy during the inelastic response will cause serious earthquake damage. During assessment it has been observed that, for low hazard level (i.e. PGA = 0.36g) earthquakes some members remains elastic which don't give clear idea of possible hysteretic energy distribution in the building. Therefore,

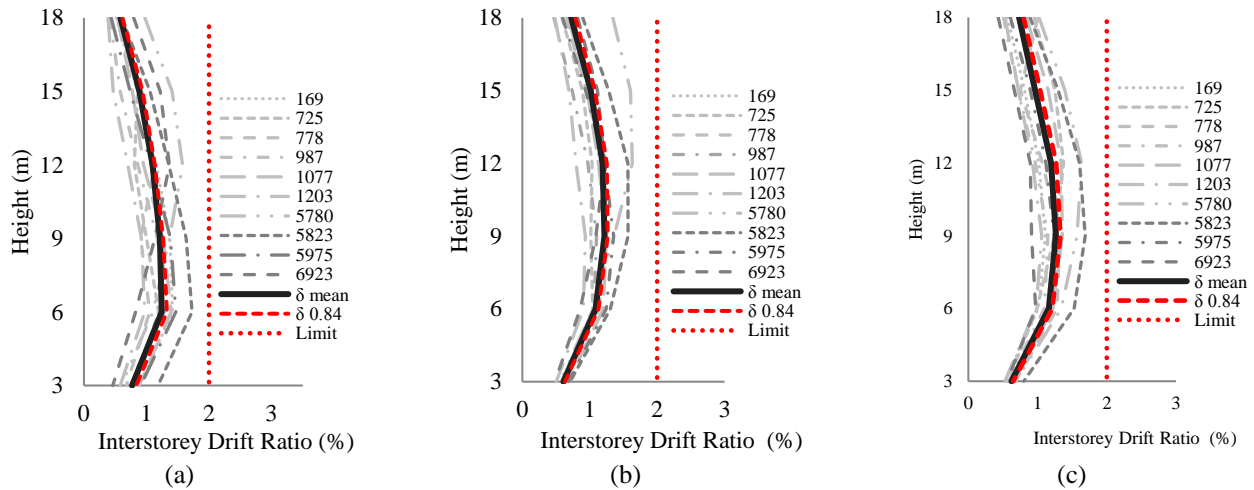


Fig. 11 Comparison of maximum inter-story drift ratio of the frame designed as per (a) FBD, (b) DDBD and (c) EBD approach for low hazard level (i.e., PGA = 0.36 g)

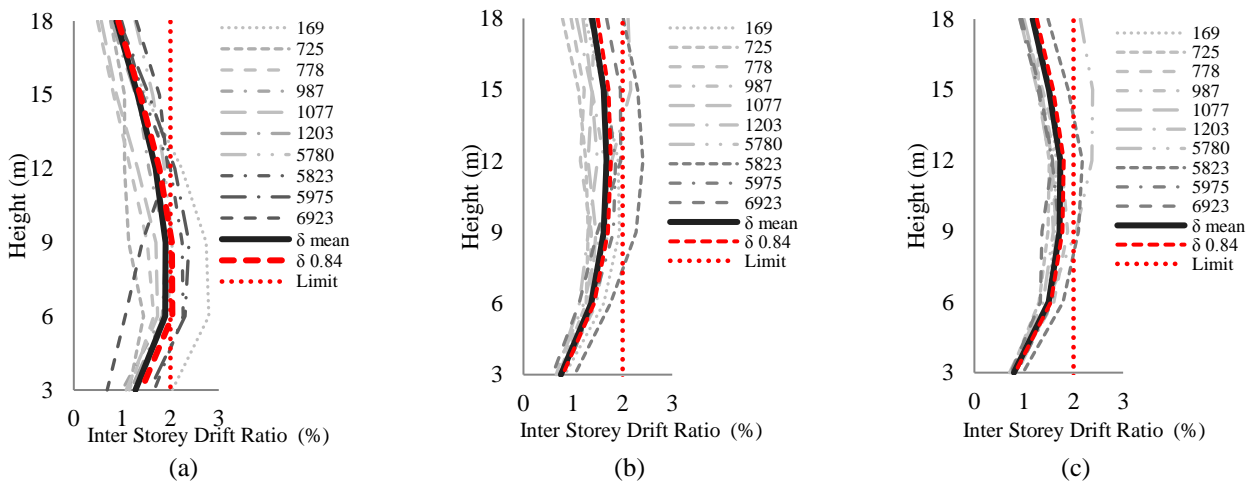


Fig. 12 Comparison of maximum inter-story drift ratio of the frame designed as per (a) FBD, (b) DDBD and (c) EBD approach for high hazard level (i.e., PGA = 0.54 g)

results of the storey hysteretic energy of the frame designed as per (a) FBD, (b) DDBD and (c) EBD approach for high hazard level (i.e., PGA = 0.54 g) have been presented (Fig. 13). Further, total input energy imparted by earthquake and subsequent hysteretic energy dissipated by frame has been summarised in Table 5. The hysteretic energy dissipated by structural components at various storey level has been calculated from the moment rotation behavior of individual hinge in seismic event. The plot of distribution of hysteretic energy at different storey level of the FBD frame (Fig. 13 (a)) shows that the upper storeys dissipate less energy than the lower ones; this indicates that larger damage will be evidenced mainly in lower stories. This major limitation of FBD frame seems to be overcome by displacement and energy based design approach. In DDBD and EBD frame considerable amount of energy has been dissipated by upper storeys than that of lower storey (Figs. 13(b) and 13(c)). Similar to the drift behavior of EBD frame relatively higher amount of energy has been dissipated by middle storey than that of DDBD frame (Fig. 13 (c)).

To understand the distribution of hysteretic energy among beams and columns of considered frames a plot of percentage component hysteretic energy over the height

has been prepared for FBD, DDBD and EBD frame (Fig. 14). Plastic deformation occurs in the columns and beams of the structure, resulting in varying degrees of damage under different PGA levels therefore representative component hysteretic energy data of ground motion record RSN 169 and RSN 987 has been considered. In case of FBD frame columns also contributes in energy dissipation at bottom as well as in upper stores along with beams. In DDBD and EBD frames also, columns participate in energy dissipation but only through strategic hinges formed at column bottom. The energy dissipated by columns in DDBD frame is relatively lesser than that of FBD frame. Apart from them, energy dissipation by the columns in upper storeys is almost insignificant and remains elastic in most of the cases. In addition to this, from Table 5 it can be observed that FBD and DDBD frame dissipate average 53 and 48 percent of total input energy through plastic action. Whereas, EBD frame dissipate average 37 percent of total input energy through plastic action. Which shows that, FBD and DDBD frame will suffer relatively more inelastic damage than the EBD frame. Which also means that in present case EBD approach provide relatively conservative design than the DDBD approach.

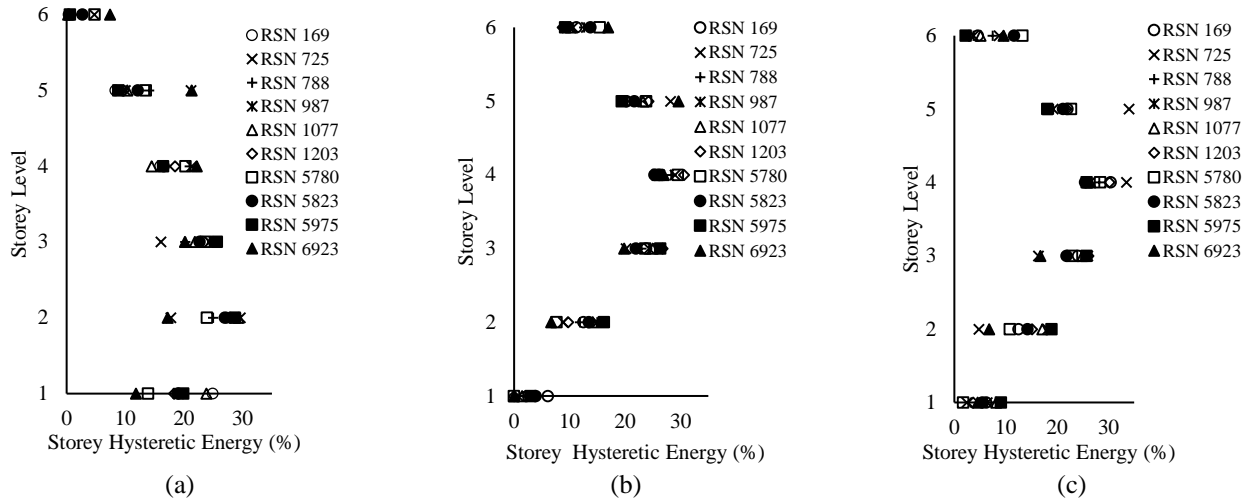


Fig. 13 Comparison of distribution of the percentage storey hysteretic energy of the frame designed as per (a) FBD, (b) DDBD and (c) EBD approach for high hazard level (i.e., PGA = 0.54 g)

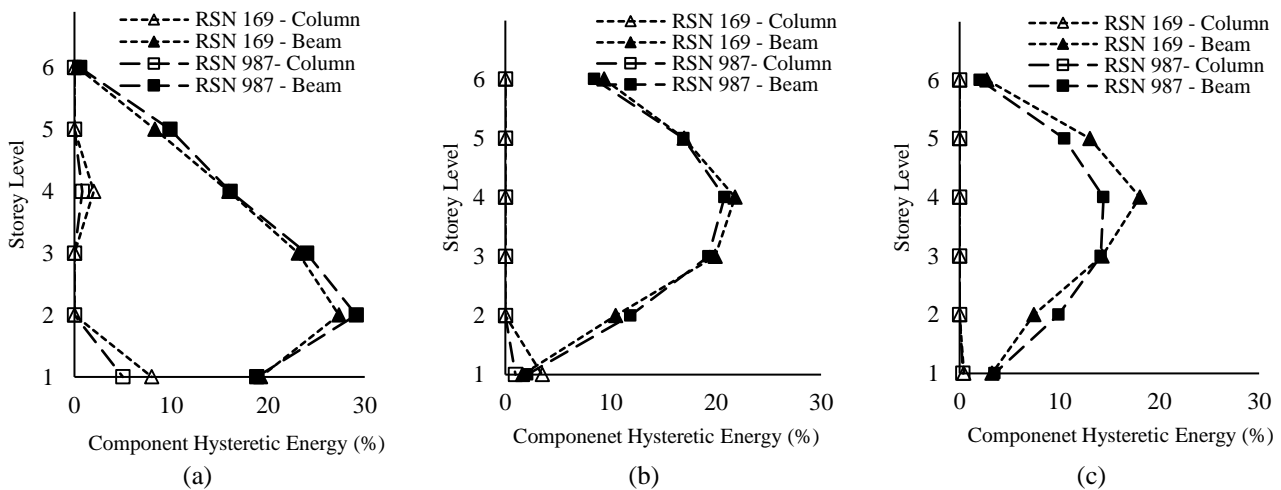


Fig. 14 Comparison of the percentage component hysteretic energy of the frame designed as per (a) FBD, (b) DDBD and (c) EBD approach for high hazard level (i.e., PGA = 0.54 g)

Table 5 Input Energy of Ground Motion and Hysteretic Energy Component of the frame designed as per FBD, DDBD and EBD approach for high hazard level (i.e., PGA = 0.54 g)

Sr. No.	Ground Motion Record	FBD		DDBD		EBD	
		Input Energy (kN-m)	Hysteretic Energy (kN-m)	Input Energy (kN-m)	Hysteretic Energy (kN-m)	Input Energy (kN-m)	Hysteretic Energy (kN-m)
1	RSN 169	1361	805	1234	674	1228	476
2	RSN 725	471	233	513	217	587	163
3	RSN 788	452	234	485	236	523	221
4	RSN 987	443	232	397	187	369	128
5	RSN 1077	457	227	447	202	482	192
6	RSN 1203	785	443	640	288	636	178
7	RSN 5780	581	339	666	339	804	386
8	RSN 5823	1441	783	1478	731	1633	744
9	RSN 5975	1007	564	844	441	629	219
10	RSN 6923	386	176	398	163	366	96

7. Conclusions

Force based design (FBD), direct displacement based design (DDBD) and energy based design (EBD) are three distinct design approaches. In present study an attempt has been made to compare these approaches using RC frame designed to satisfy a common design criterion of two percent inelastic drift. Nonlinear static (Pushover) analysis and Nonlinear dynamic time-history analysis have been used to compare seismic performance of the frame designed using the three approaches. The nonlinear analysis results show that in FBD frame, column hinges formed in different stories indicating undesirable mechanism (even though the strong column weak beam criteria has been satisfied), which is not evident in DDBD and EBD frame. Despite of considerable difference in design base shear of the three approaches, inelastic drifts obtained from nonlinear time history analysis are within the desired limit for anticipated earthquake ground motions. Beam hinge formation in DDBD and EBD frame is more evenly distributed over the height than the FBD frame. Whereas, the storey drifts of the DDBD frame is more even over the height than the EBD frame. This variation highlights that, lateral load profile and approach towards attending the global hinge mechanism also significantly influence the inelastic drift profile of structure. Finally, based on the nonlinear pushover analysis and time history analysis results it can be stated that: 1) in FBD frame plastic deformation is concentrated in the lower storey and significant hysteretic energy will be dissipated by lower storey beams and columns of the frame, 2) in EBD frame large plastic deformation is concentrated in the middle stories, inelastic hinges are well distributed over the height and hysteretic energy will be dissipated mainly by beams of the frame, and 3) in DDBD frame plastic deformation is approximately uniform over the height along with inelastic hinge formation and hysteretic energy will be dissipated mainly by beams of the frame. From the comparison of the three approaches it has been observed that DDBD and EBD approach provide better design than the FBD approach. Among EBD and DDBD approach DDBD approach is relatively simpler and frame designed by DDBD approach shows better performance.

References

- Adhikary, S. and Singh, Y. (2012), "Limitations of soil amplification provisions in the 2002 Indian seismic code", *J. Earthq. Eng.*, **16**(1), 1-14. <https://doi.org/10.1080/13632469.2011.594485>.
- Akiyama, H. (1985), *Earthquake-Resistant Limit-State Design for Buildings*. Japan: The University of Tokyo Press.
- Akiyama, H. (1988), "August. Earthquake resistant design based on the energy concept", *Proceedings of the 9th WCEE*, 905-910, Tokyo-Kyoto, Japan.
- Ancheta, T.D., Darragh, R.B., Stewart, J.P., Seyhan, E., Silva, W. J., Chiou, B.S.J. and Kishida, T. (2014), "NGA-West2 database", *Earthq. Spectra*, **30**(3), 989-1005. <http://peer.berkeley.edu/ngawest2/databases/>.
- Araújo, M., Macedo, L., Marques, M. and Castro, J. M. (2016), "Code-based record selection methods for seismic performance assessment of buildings", *Earthq. Eng. Struct. D.*, **45**(1), 129-148. <https://doi.org/10.1002/eqe.2620>.
- ASCE/SEI 41-17 (2017), *Seismic Evaluation and Retrofit of Existing Buildings*, American Society of Civil Engineers, Reston, Virginia.
- ASCE/SEI 7-16 (2016), *Minimum Design Loads and Associated Criteria for Buildings and Other Structures*, American Society of Civil Engineers, Reston, Virginia.
- ATC 19 (1995), *Structural response modification factors*, Applied Technology Council, Redwood City, California, USA.
- ATC 40 (1996), *Seismic Evaluation and retrofit of Concrete buildings*, Applied Technology Council, Redwood City, California.
- Bai, J., and Ou, J. (2012), "Plastic limit-state design of frame structures based on the strong-column weak-beam failure mechanism", *Proceedings of the 15th World Conference on Earthquake Engineering*, Lisboa, Portugal.
- Benavent-Climent, A., Pujades, L.G. and Lopez-Almansa, F. (2002), "Design energy input spectra for moderate seismicity regions", *Earthq. Eng. Struct. D.*, **31**(5), 1151-1172. <https://doi.org/10.1002/eqe.153>.
- Bommer, J.J. and Acevedo, A.B. (2004), "The use of real earthquake accelerograms as input to dynamic analysis", *J. Earthq. Eng.*, **8**(1), 43-91. <https://doi.org/10.1142/S1363246904001596>.
- Bommer, J.J. and Ruggeri, C. (2002), "The specification of acceleration time-histories in seismic design codes", *Eur. Earthq. Eng.*, **16**(1), 3-17.
- Boore, D.M. (2003), "Simulation of ground-motion using the stochastic method", *Pure Appl. Geophys.*, **160**, 635-676. <https://doi.org/10.1007/PL00012553>.
- Borzi, B. and Elnashai, A.S. (2000), "Refined force reduction factor for seismic design", *Eng. Struct.*, **22**(10), 1244-1260. [https://doi.org/10.1016/S0141-0296\(99\)00075-9](https://doi.org/10.1016/S0141-0296(99)00075-9).
- Bradley, B.A. (2011), "Design seismic demands from seismic response analyses: a probability-based approach", *Earthq. Spectra*, **27**(1), 213-224. <https://doi.org/10.1193/1.3533035>.
- Chao, S.H., Goel, S.C. and Lee, S.S. (2007), "A seismic design lateral force distribution based on inelastic state of structures", *Earthq. Spectra*, **23**(3), 547-569.
- CSI, version 20. (2017), "Integrated finite element analysis and design of structures basic analysis reference manual", *Computers and Structures Inc*, Berkeley (CA, USA).
- Dwairi, H.M., Kowalsky, M.J. and Nau, J.M. (2007), "Equivalent damping in support of direct displacement-based design", *J. Earthq. Eng.*, **11**(4), 512-530. <https://doi.org/10.1080/13632460601033884>.
- Dzadic, D., Kraus, I. and Moric, D. (2012), "Direct displacement based design of regular concrete frames in compliance with Eurocode 8", *Technical Gazette*, **19**(4), 973-982.
- EN 1998-1:2004, (2004), *Eurocode 8: Design of structures for earthquake resistance-part 1: general rules, seismic actions and rules for buildings*, Brussels: European Committee for Standardization.
- Fajfar, P. and Vidic, T. (1994), "Consistent inelastic design spectra: hysteretic and input energy", *Earthq. Eng. Struct. D.*, **23**(5), 523-537. <https://doi.org/10.1002/eqe.4290230505>.
- Fakhraddini, A. and Salajegheh, J. (2012), "Optimum automated direct displacement based design of reinforced concrete frames", *Proceedings of the 15th World Conference on Earthquake Engineering*, Lisbon, Portugal.
- FEMA 440 (2005), *Improvement of Nonlinear Static Seismic Analysis Procedure*, Federal Emergency Management Agency, Washington (DC).
- FEMA P695 (2009), *Quantification of Building Seismic Performance Factors*, Federal Emergency Management Agency, Washington (DC).
- Goel, S.C., Liao, W.C., Reza Bayat, M. and Chao, S.H. (2010),

- “Performance-based plastic design (PBD) method for earthquake resistant structures: an overview”, *Struct. Des. Tall Spec. Build.*, **19**, 115-137. <https://doi.org/10.1002/tal.547>.
- Gulkan, P. and Sozen, M.A. (1974), “Inelastic responses of reinforced concrete structures to earthquake motions”, *ACI J. Proceedings*, **71**(12), 604-610.
- HAZUS (2006), HAZUS-MH MR1/MR2, *Technical Manual*, developed by the Federal Emergency Management Agency through agreements with the National Institute of Building Sciences, Washington, D.C.
- Housner, G.W. (1956), “Limit design of structures to resist earthquakes”, *Proceedings of the 1st World Conference on Earthquake Engineering, Earthquake Engineering Research Institute*, San Francisco.
- Iervolino, I. and Cornell, C.A. (2005), “Record selection for nonlinear seismic analysis of structures”, *Earthq. Spectra*, **21**(3), 685-713.
- Iervolino, I., Maddaloni, G. and Cosenza, E. (2008), “Eurocode 8 compliant real record sets for seismic analysis of structures”, *J. Earthq. Eng.*, **12**(1), 54-90. <https://doi.org/10.1080/13632460701457173>.
- IS 456 (2000), *Plain and Reinforced Concrete – Code of Practice (Fourth Revision)*, Bureau of Indian Standards, New Delhi, India.
- IS 875-Part 1 (1987), *Code of Practice for Design Loads (other than Earthquake) for Buildings and Structures: Part 1-Dead Loads (second revision)*. Bureau of Indian Standards, New Delhi, India.
- IS 875-Part 2 (1987), *Code of Practice for Design Loads (other than Earthquake) for Buildings and Structures: Part 2-Imposed Loads (second revision)*. Bureau of Indian Standards, New Delhi, India.
- IS 1893-Part 1 (2016), *Criteria for earthquake resistant design of structures, Part 1 general provision and buildings*. Bureau of Indian Standards, New Delhi, India.
- IS 13920 (2016), *Ductile Design and Detailing of Reinforced Concrete Structures Subjected to Seismic Forces –Code of Practice (First Revision)*, Bureau of Indian Standards, New Delhi, India.
- Kappos, A.J. (1999), “Evaluation of behaviour factors on the basis of ductility and over-strength studies”, *Eng. Struct.*, **21**(9), 823-835. [https://doi.org/10.1016/S0141-0296\(98\)00050-9](https://doi.org/10.1016/S0141-0296(98)00050-9).
- Kato, B. and Akiyama, H. (1982), “Seismic design of steel buildings”, *J. Struct. Div.*, **108**(8), 1709-1721.
- Kowalsky, M.J. (1994), “Displacement based design: A methodology for seismic design applied to RC bridge columns”, M. Sc. Dissertation, University of California, San Diego.
- Kowalsky, M.J., Priestley, M.J. and Macrae, G.A. (1995), “Displacement-based design of RC Bridge columns in seismic regions”, *Earthq. Eng. Struct. D.*, **24**(12), 1623-1643. <https://doi.org/10.1002/eqe.4290241206>.
- Krawinkler, H., Medina, R. and Alavi, B. (2003), “Seismic drift and ductility demands and their dependence on ground motions”, *Eng. Struct.*, **25**(5), 637-653. [https://doi.org/10.1016/S0141-0296\(02\)00174-8](https://doi.org/10.1016/S0141-0296(02)00174-8).
- Kumar, R. and Singh, Y. (2010), “Stiffness of reinforced concrete frame members for seismic analysis”, *ACI Struct. J.*, **107**(5), 607-615.
- Kuwamura, H. and Galambos, T. (1989), “Earthquake load for structural reliability” *J. Struct. Eng.*, **128**(8), 1046-1054. [https://doi.org/10.1061/\(ASCE\)0733-9445\(1989\)115:6\(1446\)](https://doi.org/10.1061/(ASCE)0733-9445(1989)115:6(1446)).
- Lakhade S.O., Kumar, R. and Jaiswal O.R. (2018), “Damage states of yielding and collapse for elevated water tanks supported on RC frame staging”, *Struct. Eng. Mech.*, **67**(6), 587-601. <https://doi.org/10.12989/sem.2018.67.6.587>.
- Leelataviwat, S., Goel, S.C. and Stojadinovic, B. (1999), “Toward performance-based seismic design of structure”, *Earthq. Spectra*, **15**(3), 435-461. <https://doi.org/10.1193/1.1586052>.
- Loeding, S., Kowalsky, M.J. and Priestley, M.N. (1998), “Direct displacement-based design of reinforced concrete building frames”, *Report No. SSRP-98/08 Division of Structural Engineering*, University of California, San Diego.
- Massena, B., Bento, R. and Degée, H. (2010), “Direct displacement based design of a RC frame – Case of study”, *Relatorio ICIST DTC*, 0871-7869.
- Medhekar, M.S. and Kennedy, D.J.L. (2000), “Displacement-based seismic design of buildings-theory”, *Eng. Struct.*, **22**(3), 201-209. [https://doi.org/10.1016/S0141-0296\(98\)00092-3](https://doi.org/10.1016/S0141-0296(98)00092-3).
- Menon, D., Prasad, A.M. and Varughese, J.A. (2018), “Seismic Design Philosophy: From Force-Based to Displacement-Based Design”, *Adv. Indian Earthq. Eng. Seismol.*, 273-289. https://doi.org/10.1007/978-3-319-76855-7_13.
- Merter, O. and Ucar, T. (2017), “Energy-based design base shear for RC frames considering global failure mechanism and reduced hysteretic behavior”, *Struct. Eng. Mech.*, **63**(1), 23-35. <https://doi.org/10.12989/sem.2017.63.1.023>.
- Moehle, J.P. (1992), “Displacement-based design of RC structures subjected to earthquakes”, *Earthq. Spectra*, **8**(3), 403-428. <https://doi.org/10.1193/1.1585688>.
- Moghim, F. and Saadatpour, M.M. (2008), “The applicability of Direct Displacement-Based Design in designing concrete buildings located in near-fault regions”, *Proceedings of the 14th World Conference on Earthquake Engineering*, Beijing, China.
- Mukherjee, S. and Gupta, V.K. (2002), “Wavelet-based generation of spectrum-compatible time-histories”, *Soil Dynam. Earthq. Eng.*, **22**(9-12), 799-804. [https://doi.org/10.1016/S0267-7261\(02\)00101-X](https://doi.org/10.1016/S0267-7261(02)00101-X).
- Muljati I., Asisi F. and Willyanto K. (2015), “Performance of force based design versus direct displacement based design in predicting seismic demands of regular concrete special moment resisting frames”, *Procedia Eng.*, **125**, 1050-1056. <https://doi.org/10.1016/j.proeng.2015.11.161>.
- NZS 1170.5:2004 (2004), *Structural design actions: Part 5: Earthquake actions New Zealand*. Standards New Zealand, Wellington.
- Pettinga, J.D. and Priestley, M.J.N. (2005), “Dynamic behaviour of reinforced concrete frames designed with direct displacement-based design”, *J. Earthq. Eng.*, **9**(2), 309-330. <https://doi.org/10.1142/S1363246905002419>.
- Priestley, M.J.N. (2003), “Myths and fallacies in earthquake engineering, revisited”, The Ninth Mallet Milne Lecture; European School for Advanced Studies in Reduction of Seismic Risk, Rose School, Pavia, Italy.
- Priestley, M.J.N., Calvi, M.C. and Kowalsky, M.J. (2007), *Displacement-Based Seismic Design of Structures*. IUSS Press, Pavia.
- Priestley, M.J.N. and Kowalsky, M.J. (2000), “Direct displacement based seismic design of concrete buildings”, *Bulletin of the New Zealand society for Earthquake Engineering*, **33**(4), 421-444.
- SEAOC (1995), *Vision 2000: Performance-Based Seismic Engineering of Buildings*, Structural Engineers Association of California, Sacramento, California.
- Sivraj, S., Kumbhar, O. G., and Kumar, R. (2018), “Comparison of various Energy Based Approaches for Seismic Design of RC Frame Structures”, *International Conference on Advances in Construction Materials and Structures(ACMS-2018) IIT Roorkee*, Roorkee, Uttarakhand, India, March.
- Takeda, T., Sozen, M.A. and Nielsen, N.N. (1970), “Reinforced concrete response to simulated earthquakes”, *J. Struct. Div.*, **96**(12), 2557-2573.
- Vidot-Vega, A.L. and Kowalsky, M.J. (2010), “Relationship between strain, curvature, and drift in reinforced concrete moment frames in support of performance-based seismic

design”, *ACI Struct. J.*, **107**(3), 291-299.

Whittaker, A. and Rojahn, C. (1999), “Seismic response modification factors”, *J. Struct. Eng.*, **125**, 438-444.
[https://doi.org/10.1061/\(ASCE\)0733-9445\(1999\)125:4\(438\)](https://doi.org/10.1061/(ASCE)0733-9445(1999)125:4(438)).

CC